

Optical microscopic studies on grown and etched surfaces of flux grown LaAlO_3 crystals

P. N. KOTRU, ASHOK K. RAZDAN, K. K. RAINA
Physics Department, Jammu University, Jammu-180 001, India

B. M. WANKLYN
Department of Physics, Clarendon Laboratory, University of Oxford, Oxford, UK

Surface structures on as-obtained flux-grown crystals of LaAlO_3 have been investigated. Strictly oriented square, circular and rhombus shaped pointed, as well as flat-bottomed etch pits are observed. Etch pits along lineage boundaries, intersecting low-angle tilt boundaries and helical dislocations are illustrated and described. Different orientation of etch pits reveal twinning in LaAlO_3 crystals. Microdisc patterns and flux inclusions are also observed. The etch patterns on the as-obtained LaAlO_3 crystals are explained to be as a result of the flux cleaning operation of crystals in HNO_3 . Experiments on etching established HNO_3 to be a dislocation etchant for LaAlO_3 crystals. Dislocation etching kinetics of the HNO_3 - LaAlO_3 surface system are investigated for the freshly identified sites as well as for sites having a previous history of etching. Data obtained on the effects of etching time, etchant concentration and temperature on the dislocation etch rates, are analysed. The results obtained are presented and discussed.

1. Introduction

In general, the rare-earth aluminates have a structure which is only slightly distorted from that of the perfect cubic perovskite. These materials are of considerable interest on account of their magnetic and optical properties.

Flux growth of LaAlO_3 crystals has been reported by some investigators [1-9]. The structure of LaAlO_3 crystals is described by Geller and Bala [10]. Flux growth has the advantage of yielding crystals with habit faces. This makes flux-grown LaAlO_3 crystals well suited for microtopographical investigations. The flux growth of LaAlO_3 yields crystals whose growth habit is pseudocubic, four faces of which are rectangular. As mentioned in the literature, their perovskite structure deviates very slightly from cubic; the angle of the rhombohedral cell is $90^\circ 05'$.

To our knowledge, there has been no report of

a study of surface structures and etch patterns of flux-grown LaAlO_3 crystals. This paper reports results obtained on $\{100\}$ surfaces of flux grown crystals of LaAlO_3 .

2. Experimental techniques

The crystals used in the present investigation were prepared using the growth procedure as described by Garton and Wanklyn [7]. The starting composition was 5 g PbF_2 , 5 g PbO , 1 g La_2O_3 and 0.3 g Al_2O_3 . The well-mixed powder in a platinum crucible was heated to 1260°C with a soak period of 2 h, and then cooled at 2.5 K h^{-1} to 900°C . The crystals were separated by dissolving the flux in dilute acid (HNO_3 : H_2O 1:3) for 1 to 3 days at about 70°C , under a 1 A infrared lamp. (This process will be referred to as acid cleaning).

The crystals were thoroughly cleaned and then the desired surfaces coated with thin films

of silver (in most cases) in a vacuum-coating plant to enhance their reflectivity. The surfaces were then examined under a metallurgical microscope "Neophot-2" (Carl-Zeiss, Germany).

For etching LaAlO_3 crystals in the laboratory, a sealed test tube containing HNO_3 with an inclined bent tube (to ventilate out the fumes), placed in a water bath at controlled temperature, was used.

3. Results

3.1. Surface structures on as-obtained crystals

Most of LaAlO_3 crystals show evidence of having been subjected to the process of dissolution. The dissolution appears in the form of corrosion of the surface as well as in the form of selective etching. The following patterns were observed on as-obtained LaAlO_3 crystals.

3.1.1. Square, rhombus and circular etch pits

Fig. 1 is a photomicrograph of a (100) surface showing very deep and point-bottomed square-shaped etch pits as at "A", point-bottomed etch pits (not very deep) of type "B", point-bottomed square-shaped etch pits with rounded corners of type "C", small circular etch pits as at "D" and deep point-bottomed pits in pairs as at "E". The orientation of the square etch pits is as indicated in the figure. Multiple beam interferometric examination on several such surfaces revealed the depths of etch pits varying between 0.5 to 38 light waves (using green light). Pits in "pairs" (as illustrated in Fig. 2), in clusters, and pits tending to assume rhombus shape in combination with square and circular etch pits are also observed.

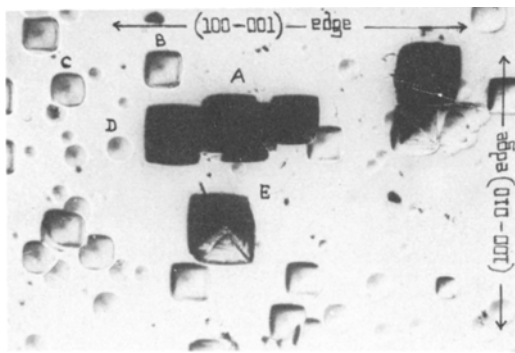


Figure 1 Square and circular etch pits on a (100) surface due to etching during the cleaning process. $\times 200$.

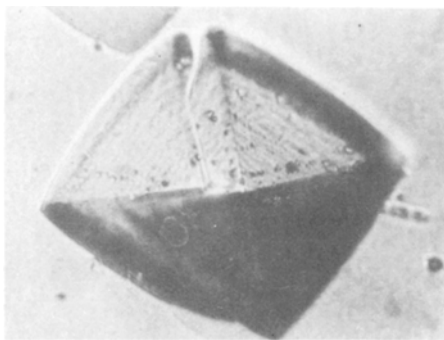


Figure 2 Etch pits in pairs on a (100) face. $\times 730$.

3.1.2. Etch pits along low-angle tilt boundaries and helical dislocations

Fig. 3 shows two rows of etch pits AB and CD on the (100) surface of an LaAlO_3 crystal. Pits in each row are equidistantly spaced which suggests their development along lineage boundaries. The formation of etch pits along low-angle tilt boundaries is further supported by the observations of three rows of etch pits intersecting to form a Y-shaped junction. Measurements along the three rows showed that the density of etch pits (n_A) in one of the rows A is equal to the sum of the densities of etch pits (n_B and n_C) in the other two rows B and C, i.e. $n_A = n_B + n_C$. The equation holds true in the case of intersecting low-angle tilt boundaries [11] between the three crystal grains forming a junction.

A row of paired etch pits along a helical dislocation [12, 13] with its axis parallel to the crystal surface, has also been observed in a number of crystals.

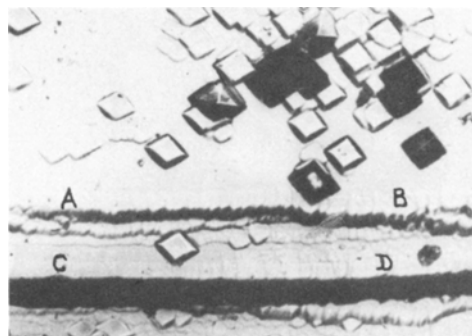


Figure 3 Lineage boundaries in LaAlO_3 crystals. $\times 200$.

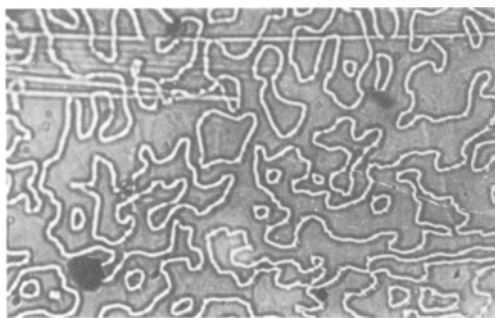


Figure 4 Inclusions in the form of irregular structures on a (100) face. $\times 350$.

3.1.3. Differently oriented etch pits (twinning)

In the case of a twinned crystal, the etch pits may either be differently shaped or differently oriented on the two sides of the boundary separating the twinned grains [14–18]. Well demarcated regions by boundaries separating etch pits differing in orientation by 91° and 95° , and also regions with differently shaped etch pits were observed on some (100) surfaces. The observations offer examples of twinning in the crystals. Interpenetrating twinned grains with no visible signs of any boundary were also observed.

3.1.4. Irregular structures

Fig. 4 shows some irregular structures observed on some surfaces. These irregular structures appear to be some solid inclusions. Such structures when observed even in combination with the etch pits on as-obtained surfaces, as shown in Fig. 5, indicate that the inclusions were not washed out during the cleaning process in HNO_3 .

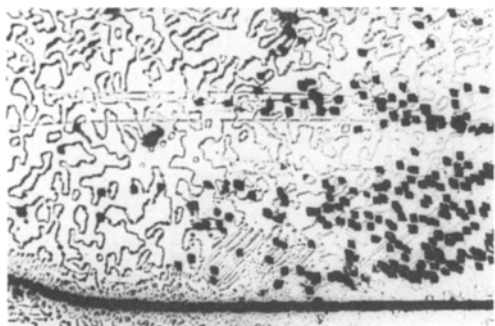


Figure 5 Inclusions in combination with etch pits on a (100) face. $\times 220$.

Experiments performed on etching of LaAlO_3 crystals in the laboratory (for details see the following sections) revealed that the irregular patterns on exposure to the etchant (boiling 100% HNO_3), are washed out after only 15 min. The experiments demonstrate that the inclusions in the form of irregular structures offer resistance to the ordinary etching conditions but cannot withstand etching by boiling 100% HNO_3 . The inclusions could be any flux material which is phased out at almost the cessation of crystal growth.

3.2.1. Etching in 100% boiling HNO_3

Experiments on etching revealed that HNO_3 is an etchant for LaAlO_3 crystals. The minimum etching time required just to nucleate the etch pits on a (100) surface is found to be 10 min. Fig. 6 shows a (100) surface etched in boiling HNO_3 for 1 h. The bigger square pits numbered in the photograph (termed “old pits”) were originally present on the surface before the crystal was etched in boiling HNO_3 . All other pits (termed “new pits”) are due to etching in boiling (100%) HNO_3 . Except for size, the so-called old pits and the new pits are identical in shape, structure and orientation.

In order to understand the mechanism of etching in 100% boiling HNO_3 , experiments on successive etching were carried out. Measurements in lateral dimensions and depth were made for both the old and the new pits at each stage of etching. The experiments led to the following observations.

1. The old point-bottomed pits show their existence at all stages of etching, whereas the flat-bottomed pits (old) were washed off

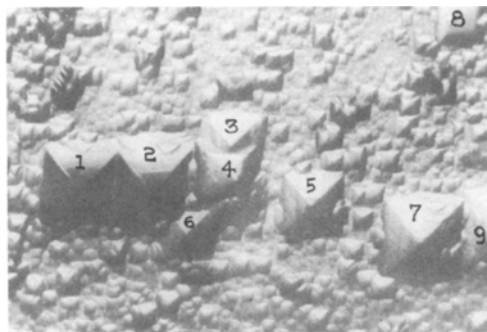


Figure 6 Etch patterns produced by boiling HNO_3 on a (100) face. $\times 140$.

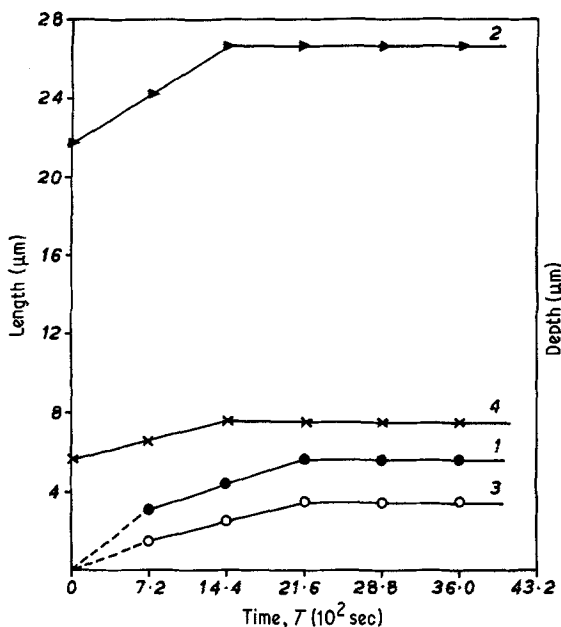


Figure 7 Graph showing lateral extension and depth of etch pits against etching time. Curves 1 and 2 show variation of lateral extension (Curve 1 for "new pits" and Curve 2 for "old pits"). Curves 3 and 4 show variation of depth (Curve 3 for "new pits" and Curve 4 for "old pits").

(observed even after only 12 min of etching) on etching.

2. The new point-bottomed pits, having developed as a result of etching by boiling HNO_3 , continue their existence and maintain their shape and orientation at all stages of etching. The new flat-bottomed pits, developed at any stage of etching, are washed off in the next stage.

The results obtained, indicate the nucleation of point- and flat-bottomed etch pits, caused by boiling HNO_3 , to be at the sites of dislocations and in some kind of superficial defects, respectively.

The data obtained on measurements of lateral dimensions (length and breadth) and depths, carried out on etching of (100) crystal surfaces in boiling 100% HNO_3 for both the old and new pits at different stages of etching, is compiled in the form of graphical analysis as shown in Fig. 7. Here it is significant to note that:

1. the variations of lateral extension and depth with etching period are linear in the cases of both the old as well as the new etch pits for only a limited period of etching; the linear dependence ceases at 14.4×10^2 and 21.6×10^2 sec etching for the old and new etch pits respectively;

2. after the "linear dependence period of etching" (14.4×10^2 sec for old pits and 21.6×10^2 sec for the new pits) is over, there is

no increase in either the lateral dimensions or the depth of etch pits (whether old or new);

3. in the region of linear dependence, the slopes give the value of $V_L = dL/dT$ to be $3.46 \times 10^{-3} \mu\text{m sec}^{-1}$ for the old pits and $1.85 \times 10^{-3} \mu\text{m sec}^{-1}$ for the new pits, respectively (Fig. 7). The velocity of etching perpendicular to the surface ($V_D = dD/dT$) as estimated from the slopes of Fig. 7 are found to be $1.38 \times 10^{-3} \mu\text{m sec}^{-1}$ for the old pits and $1.38 \times 10^{-3} \mu\text{m sec}^{-1}$ in the case of new pits.

3.2.2. Etching in different concentrations of HNO_3 at 95°C

To study the effect of concentration on the etching behaviour of LaAlO_3 crystals, several experiments on successive stages of etching, in different concentration of HNO_3 (20 to 100%) at 95°C , were performed.

Fig. 8a is a (100) crystal surface with a few old point-bottomed etch pits. Fig. 8b shows the same surface after 10 h of etching in 20% HNO_3 . It is notable that nucleation of etch pits is found all over the surface, new etch pits having developed at several sites other than those of the old ones. Both the old and the new point-bottomed etch pits continue to increase in both the lateral extensions as well as in depth as etching progresses. The etch pits, however, retain their shape and orientation at all etching stages.

Measurements of lateral extension and depth of point-bottomed pits (averaged over the

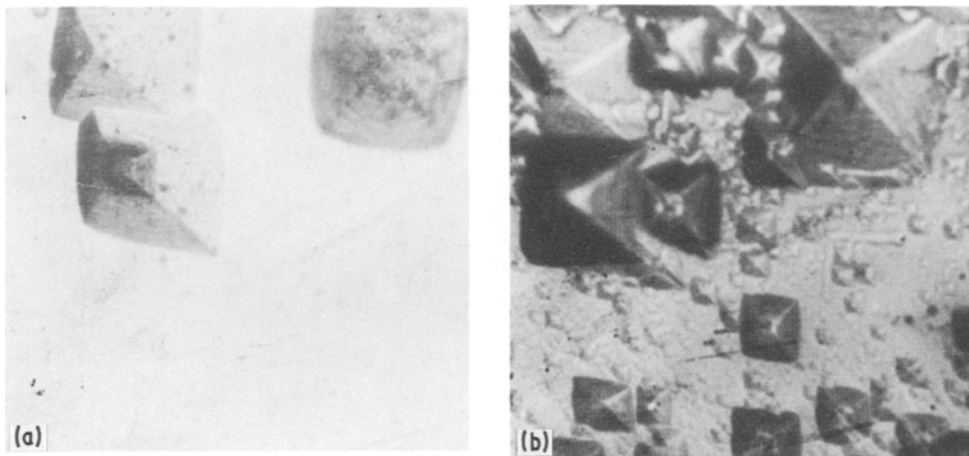


Figure 8 (a) Crystal (100) face with the "old" point-bottomed pits. (b) The surface of (a) after 10 h etching in 20% HNO_3 . $\times 500$

measurements taken on five pits) were recorded at different time intervals of prolonged etching for different etchant concentrations. The results are compiled and analysed below.

3.2.2.1. *Variation in lateral extension of pits with time.* (a) For old pits. Fig. 9 indicates dependence of length on the time of etching under different

concentrations (20 to 100%) of HNO_3 . The following points emerge.

1. At 20% HNO_3 the variation of length with time of etching is linear. The same is true for 50% concentration except in the initial short period of etching, where it shows deviation from linear dependence.
2. At concentrations above 50% (75 and

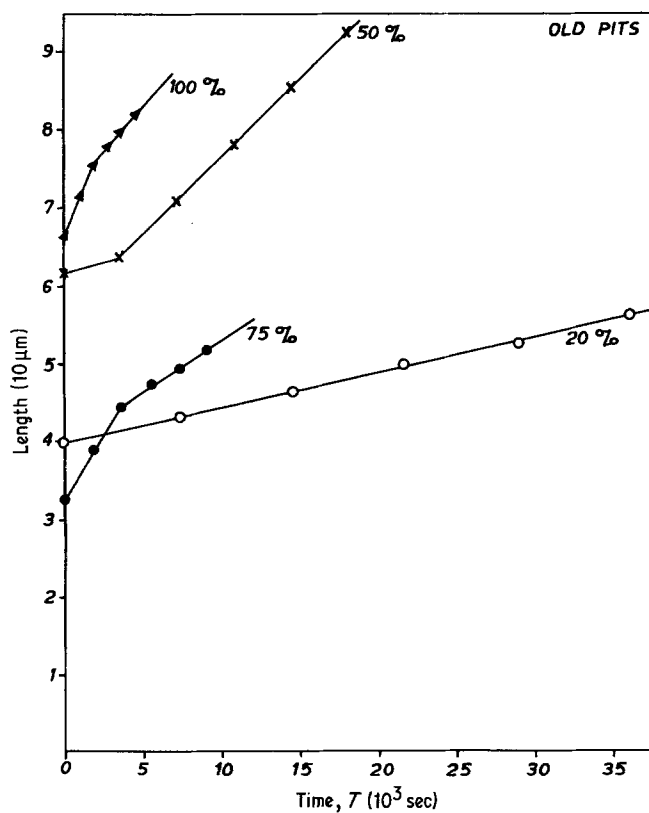


Figure 9 Plots of lateral extension of the "old pit" (due to cleaning process) against etching time for different HNO_3 concentrations (points marked \circ , \times , \bullet and \blacktriangle stand for concentrations of 20, 50, 75, and 100%, respectively).

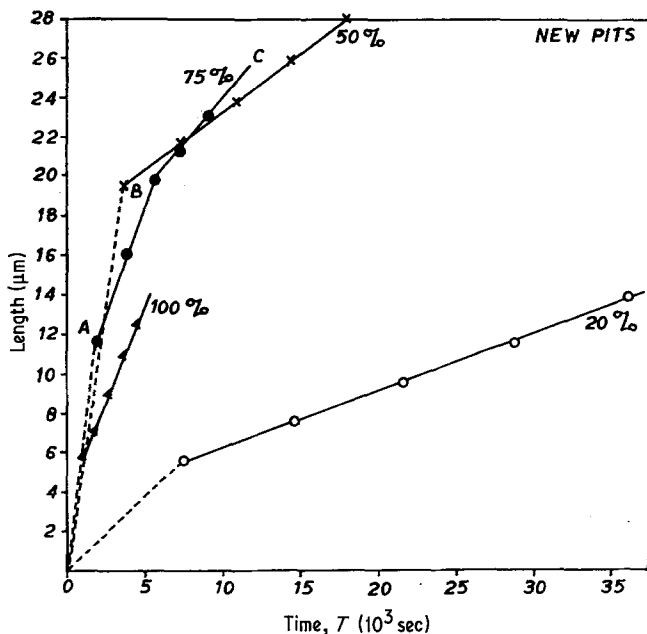


Figure 10 Plots of lateral extension of the etch pits (new) against etching time for different HNO₃ concentrations (points marked ○, ×, ● and ▲ stand for concentrations of 20, 50, 75, and 100%, respectively).

100%), the variation is linear but there is a sudden change of slope after some time of etching. In other words, the etch rates (dL/dT) in the initial periods of etching are different from the later periods of etching; the rates of etching being independent of time in each case with a transition, which is not the case with lower concentrations of 20 and 50% HNO₃. The etch rates estimated in the regions of initial and later stages of etching are compiled in Table I.

Lateral etch rates when plotted against the etchant concentration yield a curve shown in Fig. 13. (For concentrations of 75 and 100%, an average of the etch rates in the initial and later stages of etching have been considered.) The lateral etch rate increases with increase in concentrations of the etchant; the etch rate increases much more rapidly with increase in concentration after 50% HNO₃.

(b) For new pits. The data on length as recorded at different times of etching for different concentrations are shown in the graphical analysis in Fig. 10. The linear dependence of variations in length with time at concentrations of 20, 50 and 100% HNO₃ (ignoring the dotted part of the curves) is clearly indicated by the results. The curve for 75% HNO₃ shows linearity in two stages (AB and BC) with different slopes (3.4×10^{-3} and $1.4 \times 10^{-3} \mu\text{m sec}^{-1}$) in much the same way as in the case of the old pits (Fig. 9) for the same concentrations.

The variation of $V_L = dL/dT$ with etchant concentration (20 to 100% HNO₃) is depicted by a graphical analysis shown in Fig. 13. (For the curve of 75% HNO₃ an average of slopes $AB = 2.3 \times 10^{-3}$ and $BC = 0.95 \times 10^{-3} \mu\text{m sec}^{-1}$ has been taken into consideration.) The analysis indicates that the surface etch rate increases with concentration. The lateral etch rate sharply increases when concentration is increased beyond 50%.

From comparison of the results in Figs. 9 and 10, it emerges that the maintenance of time independence of lateral etch rates throughout the etching time is applicable in the low concentrations (20%) of HNO₃ both for the freshly nucleated pits as well as for the sites having an earlier history of preferential etching under different conditions. The lateral etch rate is strongly dependent on the previous history of the sample and concentration of the etchant (HNO₃), as is seen from the difference in their values in Table I. Probably, a sharp jump in the lateral etch rate above 50% HNO₃ (Fig. 13) is responsible for the deviations observed in the time independence of etch rates at higher concentrations.

3.2.2.2. Variation of pit depth with time. (a) For old pits. Fig. 11 shows the variation of depth of the old pits with time at different concentrations of the etchant. The variation is linear at all the

TABLE I Estimation of etch rates and dislocation etch pit densities

Site of etching	Etchant		Lateral etch rate, $V_L = dL/dT$ ($10^{-3} \mu\text{m sec}^{-1}$)	Vertical etch rate, $V_D = dD/dT$ ($10^{-3} \mu\text{m sec}^{-1}$)	Ratio of vertical and lateral etch rates, $d = V_D/V_L$	Average dislocation etch pit density (10^6cm^{-2})	Remarks
	Chemical formula	Conc. (%)					
Site having previous history of preferential etching (at the "old" pit)	HNO ₃	20	0.45	0.17	0.37	—	New dislocation etch pits emerge on the surface at several sites other than those of the "old" pits. Preferential etching occurs at the sites of the "old" pit also with all the etchant concentrations (20–100%). Boiling HNO ₃ produces too many flat-bottomed pits.
		50	1.93	0.57	0.29	—	
		75	2.40	1.07	0.44	—	
		100	3.5	2.0	0.57	—	
		100	3.47	1.38	1.00	—	
Site having no previous history of preferential etching (at the freshly nucleated 'new' pit)		20	0.29	0.12	0.41	15	Lower concentrations of HNO ₃ are preferable on account of steady etching. Boiling HNO ₃ leaves practically no space without etching resulting in a very high density of flat-bottomed etch pits. The surface becomes passive to etching by boiling HNO ₃ after some initial period of chemical activity at the dislocation sites.
		50	0.57	0.41	0.57	15	
		75	1.6	0.84	0.52	15	
		100	1.94	1.80	0.92	40	
		100	1.85	1.38	0.74	45	

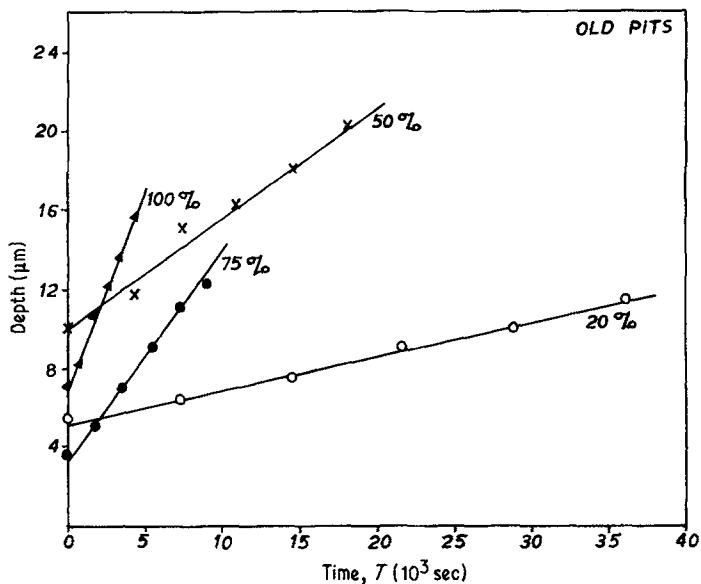


Figure 11 Graph showing variation of depth of the "old pit" with time at different concentrations of etchant (points marked O, x, ● and ▲ stand for concentrations of 20, 50, 75, and 100%, respectively).

etchant concentrations. The etch rates perpendicular to the surface estimated at different concentrations of the etchant are given in Table I.

The etch rates when plotted against the etchant concentration result in an exponential curve (curve 3) shown in Fig. 13. The logarithm of etch rates plotted against the etchant concentrations is also shown in Fig. 13 (curve 3'). The straight line represented by curve 3' in Fig. 13 confirms the exponential increase of the etch rate perpendicular to the surface with increase in etchant concentrations.

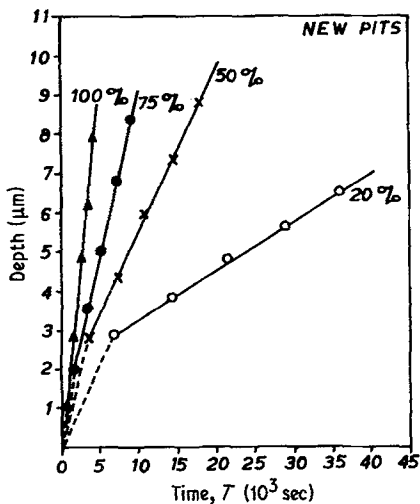


Figure 12 Graph showing variation of depth of (new) etch pits with time at different concentrations of the etchant (points marked O, x, ● and ▲ stand for concentrations of 20, 50, 75, and 100%, respectively).

(b) For new pits. Fig. 12 shows a graph of depth of the new etch pits against time of etching. Ignoring the dotted part of the curves (the time during which the dependence of depth on time is doubtful because of the factors like induction period during which an etch pit is nucleated, establishment of an equilibrium at the crystal surface etc. [19]), the variation of etch pit depth is linear in the case of all the concentrations of etchant. The slopes of the curves (Table I) yielding vertical etch rates $V_D = dD/dT$ when plotted against the etchant concentration are shown in Fig. 13 (curve 4). The shape of the curve obtained suggests an exponential type of dependence of the vertical etch rate on the etchant concentration. A graph of $\log V_D$ against etchant concentration is a straight line as expected of exponential dependence form (Fig. 13, curve 4'). In respect of the type of dependence of depth on etching time and the etchant concentration, the results are similar in nature to those of the old pits, although numerically different for obvious reasons.

4. Discussion

Most of the as-obtained LaAlO_3 crystals studied during the present investigation exhibited etch patterns on their surfaces. The etch patterns displayed include preferential etching at isolated sites leading to point- and flat-bottomed etch pits, clusters of etch pits, dislocation etch pits along low-angle tilt boundaries, differently oriented etch pits in the twinned areas and

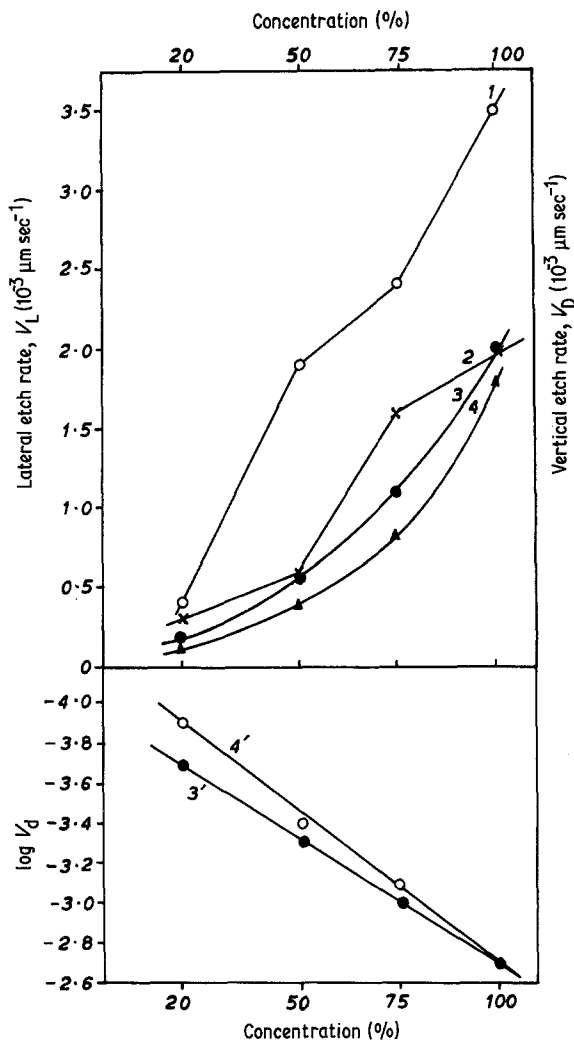


Figure 13 Graph showing dependence of lateral etch rate V_L , vertical etch rate V_D and logarithm of vertical etch rate V_D on HNO_3 concentration. Curves 1 and 2 for V_L (Curve 1 for old pits and Curve 2 for new pits). Curves 3 and 4 for V_D (Curve 3 for old pits and Curve 4 for new pits). Curve 3' and 4' for $\log V_D$ against concentration (Curve 3' for old pits and 4' for new pits).

helical dislocations. The results obtained through experiments on etching of LaAlO_3 crystals are in favour of an argument that the cleaning process in HNO_3 (for separating and cleaning crystals wrapped up in flux) is the source of etch patterns on as-obtained crystals. The cleaning process would also have tampered with any growth details on LaAlO_3 crystal surfaces.

Etching experiments on LaAlO_3 crystals in 100% HNO_3 yield interesting results. The chemical activity of the etchant ceases after some

time of initial etching only when boiling HNO_3 is used. A sudden drop of lateral as well as vertical etch rates to zero (Fig. 7) is explained to be as a result of passivity of the surface [20, 21]. Metals, particularly aluminium in this case, become passive to chemical attack by strong acids such as HNO_3 . LaAlO_3 , on reaction with HNO_3 at its boiling point (121°C), may suddenly stop being attacked after some time on account of passivity. It could be that there is a local formation of Al_2O_3 film at the sites of attack after initial reaction for some time, which may protect the surface from further etching, and thus render it passive to further attack by the etchant.

The phenomenon of passivity is not observed, in the case of HNO_3 , at a lower temperature of 95°C . This is clearly indicated by the continuous preferential etching at the defect sites and so amply demonstrated by the curves of variation of lateral extension and depth with time at different concentrations of 20 to 100% HNO_3 .

The dislocation etch rates (lateral or vertical) are strongly dependent on concentration of the etchant (Fig. 13.) Time independence of the lateral etch rate at lower concentrations (20 to 50% HNO_3) is maintained whether or not the crystal has a previous history of etching (Figs. 9 and 10). In contrast to this, the depth of dislocation etch pits varies linearly with time throughout the full range of concentration of the etchant (20 to 100%) irrespective of whether the surface has a previous history of etching or not.

Some disturbances in the rhythmic advancement of etch fronts parallel to the surface is expected due to interactions between neighbouring sources which generate them. This is likely to happen when the surface has a very high density of closely spaced sites of preferential etching. This is observed to be so at higher concentrations of HNO_3 , where the density of flat-bottomed etch pits keeps on changing at different stages of etching. This factor, however, should not ordinarily interfere much with the depth of point-bottomed etch pits where continuous digging by the etchant is not disturbed on this account. Our observations on the maintenance of time independence of the vertical etch rate at different concentrations (20 to 100% HNO_3) and an identical behaviour even on previously etched surfaces (Figs. 11 and 12) in contrast to that of lateral etch rates (Figs. 9 and

10) are significant in the light of the explanation offered.

The exponential form of dependence of the vertical etch rate at the dislocation sites of LaAlO_3 crystal surfaces on HNO_3 concentration, is indicated in the case of both the types of sites (one having a previous history of etching and the other a fresh one), as is seen in curves 3, 3', 4 and 4' of Fig. 13. This observation is also in agreement with the above explanation.

5. Conclusions

1. Flux-grown LaAlO_3 crystals are etched during the cleaning process in HNO_3 . In addition to dislocations, helical dislocations, planar defects such as low angle grain boundaries and twin boundaries, and flux inclusions are present in LaAlO_3 crystals.

2. HNO_3 is a dislocation etchant for LaAlO_3 crystals. Boiling HNO_3 does etch dislocations preferentially, but its chemical reactivity with the LaAlO_3 surface ceases after some initial period of etching due to the phenomenon of passivity.

3. The vertical etch rate is independent of etching time in HNO_3 at all concentrations in the range 20 to 100%. The increase of vertical etch rate with increase in HNO_3 concentration has characteristics of an exponential form.

4. The maintenance of time independence of lateral etch rates throughout the etching time is applicable in the lower concentrations (20%) of HNO_3 . The lateral etch rate for the " LaAlO_3 — HNO_3 " system is strongly dependent on concentration. The etch rate increases sharply after the concentration of HNO_3 exceeds 50%.

5. The lateral or vertical etch rates are dependent on the previous history of etching of the crystals.

Acknowledgements

A.K.R. and K.K.R. wish to thank the University Authorities for the award of scholarships. The work is based on a collaborative research programme between the Clarendon Laboratory, University of Oxford and the Physics Department, University of Jammu. The authors thank Dr G. Garton, Head, Crystal Growth Laboratory, Clarendon Laboratory for the encourage-

ment in the collaborative programme. We also thank Dr M. L. Kaul of the Chemistry Department for useful suggestions. The interest and co-operation of Professor N. K. Rao, Head, Physics Department, Jammu University is gratefully acknowledged.

References

1. J. D. CASHION, A. H. COOKE, J. F. B. HAWKES, M. J. M. LEASK, T. L. THORP and M. R. WELLS, *J. Appl. Phys.* **39** (1968) 1360.
2. J. D. CASHION, A. H. COOKE, M. J. M. LEASK, T. L. THORP and M. R. WELLS, *J. Mater. Sci.* **3** (1968) 402.
3. J. SIVARDIERE and S. QUEZEL, *Ambrunaz Compt. Rend* **273** (1971) 619.
4. J. P. REMEIK, *J. Amer. Chem. Soc.* **78** (1956) 4259.
5. R. C. LINARES, *J. Appl. Phys.* **33** (1962) 1747.
6. Z. N. ZONN and V. A. IOFFE, "Growth of crystals", Vol. 6-A, edited by N. N. Sheftal (Consultants Bureau, New York, 1968) p. 112.
7. G. GARTON and B. M. WANKLYN, *J. Cryst. Growth* **1** (1967) 164.
8. B. M. WANKLYN, *ibid.* **5** (1969) 323.
9. Airton Litton Industries, US Office of Naval Research-NONR-4616 (00), Advanced Research Projects Agency, ARPA 306-62.
10. S. GELLER and V. B. BALA, *Acta Crystallogr.* **9** (1956) 1019.
11. S. AMELINCKX, *Acta Metall.* **2** (1954) 848.
12. W. BONTINCK, *Phil. Mag.* **2** (1957) 561.
13. S. AMELINCKX, "The Direct Observation of Dislocations", Solid State Physics Suppl. 6 (Academic Press, New York, 1964) p. 73.
14. M. S. JOSHI and P. N. KOTRU, *Jpn. J. Appl. Phys.* **7** (1968) 700.
15. *Idem*, *Amer. Mineral* **53** (1968) 825.
16. P. N. KOTRU, A. K. JAIN and O. P. RAINA, *Ind. J. Pure Appl. Phys.* **17** (1979) 608.
17. P. N. KOTRU, Proceedings of the National Conference on Crystallography, Banaras Hindu University, Varanasi, India, February 1979, Abstract 10-18.
18. P. N. KOTRU, S. K. KACHROO and K. K. RAINA, *Kristall und Technik* **20** (1985) 27.
19. E. G. POPKOYA, G. S. MATVEEVA, A. A. PREDVODITELEV, *Kristallografiya* **14** (1969) 53.
20. G. MILAZZO, "Electrochemistry", (Elsevier, New York 1963) p. 496.
21. D. BAKER, D. C. KOEHLER, W. O. FLECKENSTEIN, C. E. RODEN and R. SABIA, "Materials technology", Physical Design of Electronic systems, Vol. II (Prentice-Hall, Englewood Cliffs, New Jersey, 1970) p. 217.

Received 27 October 1983

and accepted 20 November 1984